

# Observation of Brillouin gain spectrum in tapered polymer optical fiber

Neisei Hayashi,<sup>a)</sup> Hideyuki Fukuda, Yosuke Mizuno, and Kentaro Nakamura  
*Precision and Intelligence Laboratory, Tokyo Institute of Technology, 4259 Nagatsuta-cho, Midori-ku, Yokohama 226-8503, Japan*

(Received 27 January 2014; accepted 24 April 2014; published online 6 May 2014)

We report on the first observation of the Brillouin gain spectrum in a perfluorinated graded-index polymer optical fiber (POF) tapered by a heat-and-pull technique. The Stokes power was slightly enhanced by tapering probably on account of higher optical power density in the core. In addition, the Brillouin frequency shift was decreased by  $\sim 40$  MHz, which was experimentally verified to be partially caused by high heating temperature applied to the POF during the taper fabrication process. We anticipate that our findings will provide a basic principle of temperature sensing with “memory” function. © 2014 AIP Publishing LLC. [<http://dx.doi.org/10.1063/1.4875102>]

## I. INTRODUCTION

Brillouin scattering, one of the most important nonlinear effects in optical fibers, has been widely studied for several decades, and applied to various fiber-optic devices and systems, such as lasers,<sup>1</sup> amplifiers,<sup>1</sup> storages,<sup>2</sup> frequency-comb generators,<sup>3</sup> slow-light generators,<sup>4</sup> and distributed strain/temperature sensors.<sup>5–9</sup> Recently, Zou *et al.*<sup>10</sup> have investigated the Brillouin gain spectra (BGSs) in tapered silica single-mode fibers (SMFs) at  $1.55 \mu\text{m}$  and found that the Brillouin frequency shift (BFS) in the taper waist (outer diameter:  $5 \mu\text{m}$ ) is higher than that of the untapered silica SMF by  $\sim 270$  MHz. This report implies that the BFS in optical fibers can be controlled by adjusting the tapering conditions, which will increase the freedom in designing the above-mentioned fiber-optic Brillouin devices. Meanwhile, polymer optical fibers (POFs) have attracted a lot of attention because of their high flexibility, ease of handling, low-cost connection, and high safety;<sup>11</sup> and tapered POFs have also been extensively studied for a variety of applications.<sup>12–17</sup> However, no report has been provided on the observation of Brillouin scattering in a tapered POF yet, though the Brillouin properties in untapered POFs have already been characterized.<sup>18–20</sup> Thus, observing Brillouin scattering in a tapered POF is an important technological step toward the development of POF-based Brillouin devices with higher design freedom.

In this study, we observe the BGS in a perfluorinated graded-index (PFGI-) POF tapered by a heat-and-pull technique for the first time. The Stokes power and the BFS in the waist (outer diameter:  $223 \mu\text{m}$ ) were higher and lower (by  $\sim 40$  MHz) than those in an untapered POF, respectively. The Stokes power was enhanced because of higher optical power density in the core; whereas the BFS downshift was experimentally proved to be partially caused by the heat applied to the POF during the taper fabrication.

## II. PRINCIPLE

When injected into an optical fiber, light (or photons) interacts with acoustic phonons, generating Brillouin Stokes

light propagating in the direction opposite to the incident light. The Stokes light spectrum, called BGS, is of Lorentzian shape;<sup>1</sup> and the central frequency of the BGS is downshifted from the incident light frequency. The amount of this frequency shift is called BFS, which is  $\sim 10.8$  GHz for a silica SMF,<sup>1</sup>  $\sim 5.4$  GHz (estimated value) for a poly(methyl methacrylate)-based (PMMA-) POF,<sup>21</sup> and  $\sim 2.8$  GHz for a PFGI-POF<sup>18</sup> at  $1.55 \mu\text{m}$ . If temperature change (or strain) is applied to the fiber, the BFS shifts toward higher or lower frequency according to the fiber core material, which is the fundamental operating principle of fiber-optic Brillouin temperature (or strain) sensors. The temperature dependence coefficient of the BFS has been reported to be approximately 1.2 MHz/K for a silica SMF,<sup>22</sup>  $-7.1$  MHz/K (estimated value) for a PMMA-POF,<sup>23</sup> and  $-3.2$  MHz/K for a PFGI-POF<sup>24</sup> at  $1.55 \mu\text{m}$ . It is noteworthy that, as the strain dependence coefficient of the BFS in a PFGI-POF is  $-121.8$  MHz/‰,<sup>19</sup> the absolute value of which is about one fifth of that of a silica SMF, Brillouin scattering in a PFGI-POF has a big potential for high-precision temperature sensing with reduced strain sensitivity.

## III. EXPERIMENTAL SETUP

As a POF to be tapered in the experiment, we employed not a standard PMMA-POF but a PFGI-POF. This is because Brillouin scattering has been successfully observed only in PFGI-POFs,<sup>18</sup> which have a relatively low propagation loss of 250 dB/km even at telecom wavelength,<sup>25</sup> where mature optical devices for Brillouin detection such as amplifiers and circulators are available. The length of the POF sample was 1.0 m, and the other physical properties are summarized in Table I. The core/cladding layers and the overcladding layer were, respectively, composed of doped/undoped amorphous perfluorinated polymers (polyperfluorobutenylvinyl ether) and polycarbonate.<sup>13,25</sup>

A so-called heat-and-pull technique<sup>12–16</sup> was used to taper the POF. A chemical etching technique<sup>17</sup> is another well-known tapering method, but was not effective in tapering this type of POF because of the high chemical tolerance of its core material.<sup>25</sup> Although the core/cladding layers and the overcladding layer were different in glass-transition temperature ( $<108^\circ\text{C}$  and  $144^\circ\text{C}$ , respectively), the

<sup>a)</sup>Author to whom correspondence should be addressed. Electronic mail: hayashi@sonic.pi.titech.ac.jp

TABLE I. Physical properties of the POF sample.

Numerical aperture	Core diameter [ $\mu\text{m}$ ]	Outer diameter [ $\mu\text{m}$ ]	Core refractive index	Propagation loss [dB/km]
0.185	120	490	$\sim 1.35$	$\sim 250$

heat-and-pull technique was available on account of the relatively thin overcladding layer (see Table I). Figure 1 shows a schematic setup for tapering the POF, which contained an 80-mm-long furnace made of a U-shaped aluminum block fixed on a heater. One end of the POF was connected to a 1.55- $\mu\text{m}$  light source, and the other end was to an optical powermeter. Two regions of the POF were clamped; one was fixed to a motorized stage, and the other was connected via a spring to a force gauge fixed to another stage, with which the pulling force was monitored. A digital camera was mounted on the system to measure the waist diameter of the tapered POF. After the POF was tapered, its BGS was observed based on self-heterodyne detection detailed in Ref. 18, where the polarization state was optimized with a polarization controller.

#### IV. EXPERIMENTAL RESULTS

The furnace temperature was set to  $\sim 105^\circ\text{C}$ , which is almost the same as the glass-transition temperature of the core. The pulling velocity was approximately 0.2 mm/s, which was adaptively controlled so that the pulling force might be constantly lower than 30 mg. The tapering process was run for  $\sim 9$  min. Figure 2 illustrates a schematic diagram of the tapered POF, including three microscopic images (untapered, intermediate, and waist zones). The outer diameter of the waist was  $223 \mu\text{m}$ , corresponding to the core diameter of  $54.6 \mu\text{m}$ , which was estimated under the assumption that the ratio of the core diameter to the outer diameter remains unaltered by tapering. The elongated POF length was 102 mm (tapered length: 182 mm), and the taper ratio<sup>12</sup> was calculated to be 0.46. The total optical loss of the tapered region (excluding the propagation loss) was  $\sim 0.8$  dB, which is close to the previous report.<sup>12</sup>

Next, we cut the tapered POF at two points indicated in Fig. 2, and used the portion containing the waist zone as a sample for Brillouin measurement. The length was 121 mm, and the distribution of the outer diameter along the length measured with an optical microscope is shown in Fig. 3. The outer diameter in the  $\sim 60$ -mm-long waist zone was almost constant ( $\sim 225 \mu\text{m}$ ). One end of the sample (relative position = 0 mm in Fig. 3) was flatly polished, and butt-coupled to a silica SMF.<sup>18</sup>

Figure 4 shows the BGS of the tapered POF measured at  $17^\circ\text{C}$  in which that of the untapered POF (same length, i.e.,

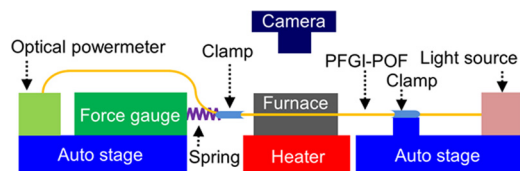


FIG. 1. Schematic setup for POF tapering by heat-and-pull technique.

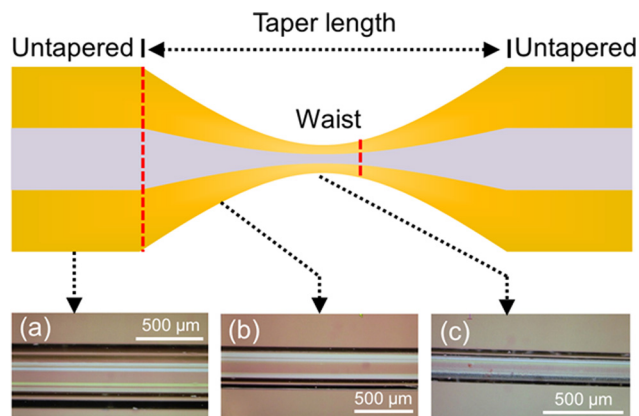


FIG. 2. Schematic structure of the tapered POF, along with the photographs of (a) untapered, (b) intermediate, and (c) waist zones. The red dotted lines indicate the positions at which the sample was cut for Brillouin measurement.

121 mm) is also displayed for comparison. The incident optical power was set to as high as 30 dBm (=1 W), because the Brillouin scattering signal from such a short POF is extremely small.<sup>18</sup> The Stokes power of the tapered POF was only slightly ( $\sim 0.1$  dB) higher than that of the untapered POF, which does not agree with our calculation ( $>4$ -dB enhancement) taking optical power density into consideration;<sup>26,27</sup> this is because the Stokes power is so small that the influence of the noise floor and the polarization-dependent fluctuations are extremely large. The BFS of the tapered POF was downshifted from that of the untapered POF by  $\sim 40$  MHz. The sign and absolute value of this BFS shift were opposite to and smaller than that of the tapered silica SMF ( $\sim 270$  MHz), respectively.<sup>10</sup>

Finally, to study the origin of the BFS shift caused by tapering, we measured the BGSs in the same untapered POF sample (used as a reference in the preceding experiment) in the following three sequential conditions: (i) at room temperature ( $15^\circ\text{C}$ ), before heating; (ii) heated at  $112^\circ\text{C}$ , kept for 5 min; and (iii) cooled at room temperature ( $15^\circ\text{C}$ ), kept for 5 min. As shown in Fig. 5, the BFSs were approximately 2.84 GHz for (i), 2.53 GHz for (ii), and 2.76 GHz for (iii). As

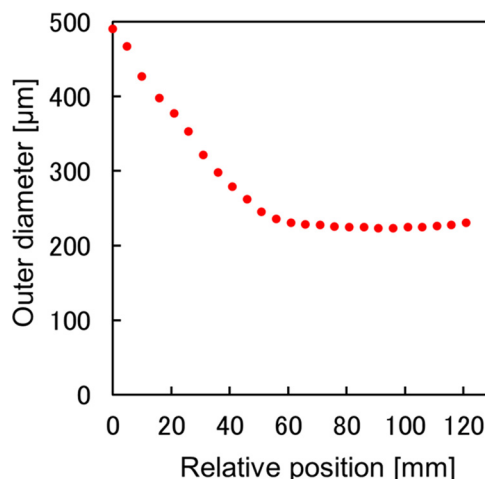


FIG. 3. Measured outer diameter as a function of relative position along the tapered POF.

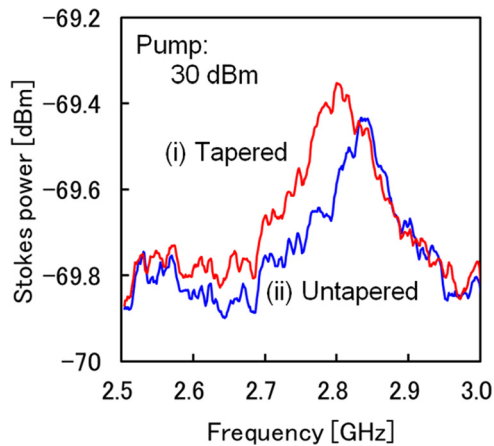


FIG. 4. Measured BGSs in POFs: (i) tapered and (ii) untapered.

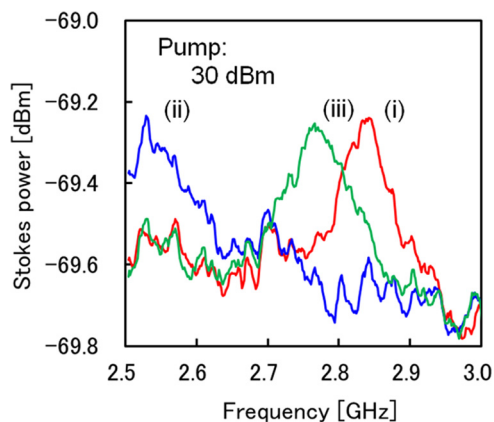


FIG. 5. Measured BGSs in POF: (i) at room temperature (15°C), before heating; (ii) heated at 112°C, kept for 5 min; and (iii) cooled at room temperature (15°C), kept for 5 min.

the POF sample was untapered, the  $\sim 80$ -MHz downshift of the BFS from (i) to (iii) appears to be caused not by the pulling process but by the applied high heating temperature comparable to the glass-transition temperature of the core material, which may induce polymer transformation<sup>28</sup> as well as dopant diffusion.<sup>29,30</sup> Note that such BFS shifts have not been observed in previous reports that investigate the BFS dependence on temperature ranging up to 80°C.<sup>19,24</sup> However, since the BFS was downshifted in this experiment by twice the amount in the tapered POF, we speculate that the amount of the BFS shift after tapering is dependent not only on the heating temperature and duration but also on mechanical deformation, on which further detailed study is required. We might control the BFS in POFs by properly adjusting these conditions in future.

## V. CONCLUSION

By the heat-and-pull technique, we fabricated the PFGI-POF taper with an outer diameter of the waist of 223  $\mu\text{m}$ , and successfully observed its BGS for the first time. The Stokes power was slightly enhanced by tapering probably because of higher optical power density in the core. The BFS was downshifted by  $\sim 40$  MHz, which was experimentally shown to

originate partially from the heat applied to the POF. By using the enhanced Brillouin signal in a much longer tapered POF, the signal-to-noise ratio of the POF-based distributed sensing systems could be improved. In addition, the BFS shift induced by high heating temperature might be actively utilized as a principle of the “temperature memory effect.” We believe that, along with the previously reported “strain memory effect,”<sup>31</sup> this novel function could be of great use in implementing POF-based Brillouin devices and systems including distributed strain and temperature sensors.<sup>5–9</sup>

## ACKNOWLEDGMENTS

This work was partially supported by a Grant-in-Aid for Young Scientists (A) (No. 25709032) from the Japan Society for the Promotion of Science (JSPS), and by research grants from the General Sekiyu Foundation, the Iwatani Naoji Foundation, and the SCAT Foundation. N.H. acknowledges a Grant-in-Aid for JSPS Fellows (No. 25007652).

- <sup>1</sup>G. P. Agrawal, *Nonlinear Fiber Optics* (Academic Press, California, 1995).
- <sup>2</sup>Z. Zhu, D. J. Gauthier, and R. W. Boyd, *Science* **318**, 1748 (2007).
- <sup>3</sup>G. J. Cowle, D. Yu, and Y. T. Chieng, *J. Lightwave Technol.* **15**, 1198 (1997).
- <sup>4</sup>K. Y. Song, M. G. Herraes, and L. Thevenaz, *Opt. Express* **13**, 82 (2005).
- <sup>5</sup>T. Horiguchi and M. Tateda, *J. Lightwave Technol.* **7**, 1170 (1989).
- <sup>6</sup>T. Kurashima, T. Horiguchi, H. Izumita, S. Furukawa, and Y. Koyamada, *IEICE Trans. Commun.* **E76-B**, 382 (1993).
- <sup>7</sup>D. Garus, K. Krebber, F. Schliep, and T. Gogolla, *Opt. Lett.* **21**, 1402 (1996).
- <sup>8</sup>K. Hotate and T. Hasegawa, *IEICE Trans. Commun.* **E83-C**, 405 (2000).
- <sup>9</sup>Y. Mizuno, W. Zou, Z. He, and K. Hotate, *Opt. Express* **16**, 12148 (2008).
- <sup>10</sup>W. Zou, W. Jiang, and J. Chen, *Opt. Express* **21**, 6497 (2013).
- <sup>11</sup>M. G. Kuzyk, *Polymer Fiber Optics: Materials, Physics, and Applications* (CRC, Boca Raton, 2006).
- <sup>12</sup>R. Gravina, G. Testa, and R. Bernini, *Sensors* **9**, 10423 (2009).
- <sup>13</sup>C. Pulido and O. Esteban, *Sens. Actuators B* **157**, 560 (2011).
- <sup>14</sup>C. Beres, F. V. B. de Nazare, N. C. C. Souza, M. A. L. Miguel, and M. M. Werneck, *Biosens. Bioelectron.* **30**, 328 (2011).
- <sup>15</sup>Y. M. Wong, P. J. Scully, R. J. Bartlett, K. S. C. Kuang, and W. J. Cantwell, *Strain* **39**, 115 (2003).
- <sup>16</sup>A. Brockmeyer, J. Coutandin, W. Groh, T. F. Stehlin, and J. Theis, *Appl. Opt.* **31**, 746 (1992).
- <sup>17</sup>D. F. Merchant, P. J. Scully, and N. F. Schmitt, *Sens. Actuators A* **76**, 365 (1999).
- <sup>18</sup>Y. Mizuno and K. Nakamura, *Appl. Phys. Lett.* **97**, 021103 (2010).
- <sup>19</sup>Y. Mizuno and K. Nakamura, *Opt. Lett.* **35**, 3985 (2010).
- <sup>20</sup>N. Hayashi, Y. Mizuno, and K. Nakamura, *Opt. Express* **20**, 21101 (2012).
- <sup>21</sup>N. Hayashi, Y. Mizuno, D. Koyama, and K. Nakamura, *Appl. Phys. Express* **4**, 102501 (2011).
- <sup>22</sup>T. Kurashima, T. Horiguchi, and M. Tateda, *Opt. Lett.* **15**, 1038 (1990).
- <sup>23</sup>N. Hayashi, Y. Mizuno, D. Koyama, and K. Nakamura, *Appl. Phys. Express* **5**, 032502 (2012).
- <sup>24</sup>K. Minakawa, N. Hayashi, Y. Shinohara, M. Tahara, H. Hosoda, Y. Mizuno, and K. Nakamura, *Jpn. J. Appl. Phys.* **53**, 042502 (2014).
- <sup>25</sup>Y. Koike and M. Asai, *NPG Asia Mater.* **1**, 22 (2009).
- <sup>26</sup>D. Iida and F. Ito, *J. Lightwave Technol.* **26**, 417 (2008).
- <sup>27</sup>D. Marcuse, *Bell Syst. Tech. J.* **56**, 703 (1977).
- <sup>28</sup>J. Saneyoshi, Y. Kikuchi, and O. Nomoto, *Handbook of Ultrasonic Technology* (Nikkan Kogyo, Tokyo, 1978).
- <sup>29</sup>K. Lyytikäinen, S. Huntington, A. Carter, P. McNamara, S. Fleming, J. Abramczyk, and G. Schotz, *Opt. Express* **12**, 972 (2004).
- <sup>30</sup>M. Asai, R. Hirose, A. Kondo, and Y. Koike, *J. Lightwave Technol.* **25**, 3062 (2007).
- <sup>31</sup>K. Nakamura, I. R. Husdi, and S. Ueha, *Proc. SPIE* **5855**, 807 (2005).